JOURNAL OF PROPULSION AND POWER
Vol. 14, No. 5, September–October 1998

Liquid-Propellant Rocket Engine Health-Monitoring Techniques

Yulin Zhang,* Jianjun Wu,† Minchao Huang,‡ Hengwei Zhu,‡ and Qizhi Chen§
National University of Defense Technology, Changsha, Hunan 410073, People's Republic of China

Health monitoring of liquid-propellant rocket engines (LRE) is one of the key technologies for improving the safety of existing engines and developing reliable next-generation engines. Extensive research has been done on the health monitoring of the Space Shuttle Main Engine and next-generation reusable LRE. A brief overview of these research projects is presented. Research advances on the health monitoring of the Long March Main Engine YF-20B are described in detail. The failure mode simulation and analysis of the YF-20B engine are introduced. A component module-based diagnosis method is developed, and a fuzzy hypersphere neural network is demonstrated for the fault detection and isolation of the engine. A real-time verification system for the health-monitoring algorithms and system was constructed and applied in the research.

I. Introduction

BECAUSE of increasingly stringent requirements for the safety, reliability, and operational capabilities of space vehicles and their launch systems in the past 30 years along with the feasibility provided by the progress of modern science and technology, the health-monitoring techniques for liquid-propellant rocket engines (LRE) have undergone significant developments.

In earlier stages of development, health-monitoring technology was applied in the ground test process for large-scale LRE. In the 1970s, expendable LREs, such as Atlas and Titan, were monitored by redlines, which are limits or thresholds on some important operating parameters,[1] and automatic test data analysis systems were progressively developed for these engines in early 1990s.[2] The partially reusable rocket engine Space Shuttle Main Engine (SSME), developed in the 1970s, is monitored by a condition-monitoring system that is a simple function of redlines.[3] In the 1980s the SAFD (System for Anomaly and Failure Detection) was developed for SSME ground tests to improve the monitoring performance of the redline system.[1] To develop higher-performance health-monitoring systems for SSME and next-generation reusable rocket engines, health-monitoring systems, such as HMS (Health Monitoring System),[3] HMSRE (Health Management System for Rocket Engine),[1] IHM (Integrated Health Monitoring),[4] and ICS (Intelligent Control System)[1,5,6] were proposed and studied intensively from the late 1980s to the early 1990s. The operations coverage of the health-monitoring techniques was extended from ground test to flight and postflight evaluation. The high-thrust rocket engines developed in the former USSR, such as the RD-170, RD-120, and RD-0120, were equipped with TDS (Technology Diagnostic Systems) in the 1980s. The TDS evaluates the operational health of the engine during the ground test and postflight through detecting and diagnosing the static and dynamic parameters.[7,8]

From the preceding statement it can be seen that the upward trend of continuously increasing requirements for the health monitoring of propulsion systems is increasingly urgent. In the past 30 years an enormous development and wide application of correlative scientific theory and advanced technology has responded to these requirements. The theories and methods of emerging science and technologies such as computer science, automatic control, signal processing, system identification, artificial intelligence, and special sensor technology are exploited abundantly in the course of developing and studying health-monitoring systems for liquid rocket propulsion systems. These techniques have been applied successfully to fault detection and diagnosis (FDD) in fields such as machinery, electronic systems, chemical engineering, aviation, and nuclear power. Thus, some relevant experience is available for the development of health-monitoring techniques for space vehicles and liquid rocket propulsion systems.

Health monitoring of LRE has become one of the key technologies for improving the safety of current engines and for developing a new generation of reliable engines. FDD technologies play a very important role in the health monitoring of LRE. Therefore, research work has focused on the adequacy of detection and diagnosis algorithms. To provide an overall description of theoretical research on and application of health-monitoring technology to LRE, the structure, systems, and algorithms of health monitoring will be reviewed in the following sections. Some research advances on the health monitoring of the YF-20B engine are described in detail.

II. Principles of Health Monitoring

Failures of LRE can be divided into slow and urgent categories. Slow failures, such as wearing of gears and propellant leaks, can result in the deterioration of engine performance, but urgent failures, such as leaking of fuel into the oxidizer pump, may lead to the explosion of an engine. Health-monitoring technology of LRE can provide fault alarms or control capacity for propulsion systems to ensure mission success and prevent the loss of life and destruction of facilities because of disastrous failures. Health-monitoring systems for LRE consist of fault detection, diagnosis, decision making, and fault control.

Fault detection can be conducted through analysis of measurements from special sensors and computational algorithms. Much effort has been made to increase detection sensitivity while reducing the possibility of false alarms.

The function of fault diagnosis algorithms is to recognize the failure type, locate the failure position, and determine the failure extent. Detecting and diagnosing processes may be combined in one algorithm.

Received Sept. 2, 1997; revision received Feb. 13, 1998; accepted for publication April 1, 1998.

*Professor, Department of Space Technology. E-mail: zyl@nudt.edu.cn. Member AIAA.
†Associate Professor, Department of Space Technology.
‡Doctoral Student, Department of Space Technology.
§Professor, Department of Space Technology.

According to the diagnostic results the decision-making algorithm evaluates the developing trend and the influence of the failure on the engine operation conditions. Fault control action is then introduced to shut down the engine, reduce the thrust level, or switch to redundant systems.

Because of the extreme complexity of the dynamic process and strong random disturbances in the operation of LRE, it is difficult to model the engine system accurately. Therefore, detection and diagnosis algorithms must be designed to be robust in terms of model uncertainties and random disturbances, that is, to be sensitive to faults with a very low false-alarm possibility. To maintain the inherent reliability of a rocket engine, it is required that its health-monitoring system not be incorporated into the engine hardware. Research on algorithms for fault detection and the diagnosis of LRE has also focused on real-time abilities to increase the response speed of the algorithm.

III. Overview of Health Monitoring Systems

The technical development of health monitoring LRE mainly includes system architecture, sensor technology, and algorithms. A brief overview of these three aspects of health-monitoring research will be given in this section.

A. System Architecture

Since mid-1980, many health-monitoring system architectures have been proposed and developed, and many of them have tried to improve the health monitoring of SSME.

The SAFD system was studied and applied to improve the fault-detection ability of the SSME ground test process.[1] SAFD is suitable for fault detection during main-stage operation of SSME. The average value of every measured parameter is calculated in a statistical window, and 23 parameters were selected for monitoring. A shutdown command will be given if the average parameters of any four sensors exceed their threshold during engine operation. Because of the much narrower threshold used in SAFD, the detection response and reliability of SAFD are much better than those of redlines. Reference 1 also developed the Flight Accelerometer Safety Cutoff System and model-based algorithms, and ran these algorithms in parallel with SAFD during the monitoring of SSME. This health-monitoring system architecture is HMSRE.[1]

The HMS was proposed to enhance the monitoring performance of SSME.[3] The HMS consists of five functional subsystems, namely, health monitoring, test data recording, off-line data analysis, database, and system communication. The system architecture is of three levels. Three detection algorithms, ARMA (Auto-Regression Moving Average), RESID (Recursive Structural Identification), and Cluster, are used in the first level to process sensor data in parallel. The health condition of engine components are evaluated according to the outputs of the first level, and the health condition of the whole engine system is evaluated in the third level.

The PTDS is a posttest diagnostic system for the SSME.[9] It is a general automatic posttest or postflight data processing system for rocket engines. The IHM was developed for expendable and reusable rocket engines.[4] Its systemic monitoring concept includes manufacturing health monitoring, ground health monitoring, and vehicle health monitoring.

The ICS synthesizes fault detection, diagnosis, and multivariable control techniques for the health management of liquid-propellant rocket engines.[1,5,6,10] It was proposed and studied for the SSME and next-generation reusable rocket engines. The engine operation parameters, such as thrust, mixture ratio, turbopump rotation speed, and high-pressure turbine temperatures are considered to be controlled variables. Engine detection and diagnostic results are used to drive the multivariable control system to control thrust level or reconstruct the propulsion system. ICS is a very useful concept for improving the flexibility, operability, and availability of next-generation reusable propulsion systems.

B. Sensor Techniques

Sensor technique is the basis of the health monitoring of LRE. Firstly, all of the detection and diagnostic results of algorithms depend on data from sensors and, secondly, specially developed sensors can be used for the direct health evaluation of engine components.

Reference 3 evaluated 30 sensor technologies that may potentially be used in SSME health monitoring. Among them are eight easily available technologies: plume spectroscopy, acoustic emission, optical pyrometer, solid-state leak sensor, polyvinylidene fluoride sensor, plume electrical diagnostics, fiber-optic deflection meter, and a laser vibration sensor. Reference 11, for example, successfully developed a plume spectroscopy diagnostic system, the Optical Plume Anomaly Detector (OPAD), and applied it in their ground test facilities.

Reliable fault detection and diagnosis require data provided by sensors. However, the possibility of sensor anomaly is sometimes much higher than that of the engine components. Therefore, sensor fault detection and diagnosis are of great importance and there has been significant research on this subject.[12,13]

C. Algorithms for FDD

FDD algorithms process signal data and evaluate the health conditions of the engine system. The construction of these algorithms can be based on the mathematical model of an engine system or on the experience of experts.

1. *Model-Based Algorithms*

Mathematical models of the engine system can be developed from the principle of the dynamic process in the engine system. The difference between the model output and the engine sensor output is taken as the residual. FDD decisions are made by means of statistical or logical processing of the residuals. The RESID is a nonlinear static modeling algorithm for detection for the SSME startup.[3] The ARMA algorithm for the detection for the main stage of the SSME models the engine parameters with the auto-regression moving average method.[3] A power balance model was used in Ref. 14 to develop a real-time monitoring algorithm for the SSME. The higher-order state-space model was also used to construct detection and diagnosis algorithms by means of state estimation or parameters identification.[15]

2. *Pattern Recognition*

The main task of the failure detection is to distinguish between nominal and abnormal situations, so that pattern-recognition-based diagnosis systems can be derived.[16] A pattern-recognition-based detection algorithm was developed for the main-stage monitoring of SSME.[3]

3. *Artificial Neural Networks*

Artificial neural networks have the advantages of associative memory, self-learning, adaptive ability, self-organization, strong robustness, and parallel processing. Therefore, they can play an important role in the monitoring algorithms for liquid-propellant rocket engines.[17,18] Radial basis function classifier networks were developed to predict element concentration and combustion temperature in a plume spectrum.[19]

4. *Expert Systems*

Expert system algorithms apply human experts' experience to the detection and diagnosis of rocket engines. Reference 20 developed a health-monitoring expert system, THAES (Titan Health Assessment Expert System), for the automatic posttest evaluation of the first-stage engines of Titan. THAES was constructed in "if-then" rules, among which are 42 rules for detection and 48 rules for diagnosis. Expert system algorithms were also developed for detection and diagnosis in the SSME.[21,22]

IV. Research on the Health Monitoring of the YF-20B Engine

The Long March Main Engine, YF-20B, is a gas-generator cycle engine with a UDMH/N_2O_4 propellant combination. The health monitoring of the YF-20B engine is of great importance for the enhancement of the safety and reliability of the launch vehicle series.

A. Fault Simulation and Analysis

The failure modes and failure response characteristics of LRE are the fundamental bases for the study of FDD methods. Because of the cost and danger of failure tests, it is not realistic to acquire enough test data under many fault conditions solely through tests. Thus, LRE fault simulation and analysis play an important role in the study of FDD of LRE.

1. Mathematical Models of YF-20B Engine

The LRE is a complicated thermodynamic and hydrodynamic mechanical device. In general, the failure modes of the operating process can be divided into two general categories: Fluid pipeline system failures and mechanical failures. These failure effects can be displayed by changes in the LRE's performance and thermodynamic parameters.[23] In this paper, emphasis is placed on studying the FDD methods based on the thermodynamic and hydrodynamic parameters. Therefore, a discussion of the fundamental principles of the engine-operating process and its mathematical models is first presented, and the main failure modes of the YF-20B engine are then described.

The YF-20B engine is a pump-fed system driven by a gas generator as shown in Fig. 1. In the diagram the control gas lines and pressurization system lines are not shown and they are not considered in the mathematical models.

The mathematical model is the basis of the study of LRE health-monitoring techniques. These models include static nonlinear models, dynamic nonlinear models, and other models suitable for different purposes, such as real-time simulating models, filter-designing models, and parameter-estimation models. Thus, much attention has been paid to and significant effort has been expected on the building of models.

By the comprehensive use of engine pipeline equations, turbopump equations, and thrust chamber equations, the lumped parameter models of the YF-20B engine have been developed.[24] According to the requirements, the static nonlinear models (including fault factors) are set up for static fault effect simulation, linear fault isolation methods study, and analysis of sensitivity of the parameters measured. Also established are the dynamic nonlinear models (including fault factors) for fault transient performance simulation, fault mode identification and verification, faulty dynamic data production, filter design model production, etc. A real-time fault simulation model is used for the real-time verification system.

2. YF-20B Engine Failure Modes and Effect Analysis

Failure mode analysis mainly includes the statistical analysis for the main failure types and the probability of occurrence, the selection and evaluation of monitored parameters, the analysis of the monitored parameters' sensitivity to faults, and the response characteristics of the monitored parameters to failure. Both test data statistics and numerical simulation methods are used in the failure mode analysis.

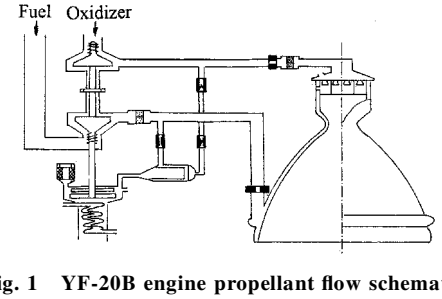

Fig. 1 YF-20B engine propellant flow schematic.

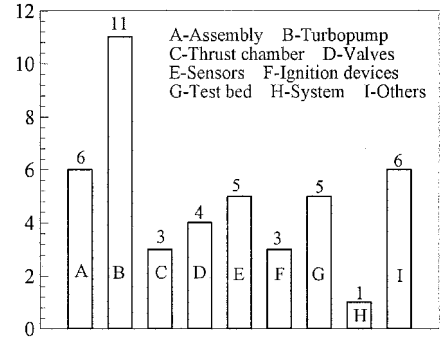

Fig. 2 Statistical results of failure types of YF-20B engine.

The historical test data of the YF-20B engine show that the main failures of YF-20B include turbopump system failure, valve failure, pipeline failure, and thrust chamber failure. The failure modes include leakage at joints, rupture of turbine blades, damage of shafts and bearings, fracture of ducts, failure of seals, operating anomalies in valves, superfluous inclusion, and ablation of components. The statistical results of test failures of the YF-20B engine are shown in Fig. 2.[25]

It can be seen that the turbopump system failure is the most likely to fail. Therefore, emphasis should be placed on turbopump fault detection and diagnosis for the YF-20B engine.

To carry out fault detection and diagnosis of LRE, not only should the main failure modes of engine be well known but also the measured response of signals to a variety of failure modes should be identified.

The operating conditions of LRE are described by a number of thermodynamic and hydrodynamic parameters, but the sensitivities of these parameters to operating conditions are very different. In fact, the number of parameters monitored in practical operations are very limited. Thus, to build a reliable and effective LRE condition monitoring system, careful selection and evaluation of these monitored parameters are necessary. Three criteria for the selection and evaluation of monitored parameters were proposed in our studies: The response of parameters to external and internal disturbances, the signal-to-noise ratio (SNR) in engine environment, and transient features under faulty conditions.

In Table 1 the average value ($\bar{X}$) and noise amplitude (ΔS) of the measured parameters of the YF-20B engine are computed statistically for 30-s intervals during a normal main-stage test. Evidently, the pressures at the inlets of the oxidizer and fuel pumps are not suitable as monitoring parameters, whereas the temperature at the turbine inlet is quite acceptable for monitoring.

In addition, the response of parameters to external and internal disturbing factors and the sensitivity of the parameters to fault conditions were analyzed through mathematical simulations.[25]

B. Diagnosis Methodology Based on Component Module for Main-Stage Operation

A liquid-propellant rocket engine is composed of various components linked to one another: Pipes, pumps, combustion chamber, etc. The output of a component is determined by the input into it. In the main-stage operation of a liquid-propellant rocket engine, the relation between the input and the output can be described by the static character equation

$$\boldsymbol{Y}_{\text{out},j} = \boldsymbol{C}_j(\boldsymbol{Y}_{\text{in},j}) \tag{1}$$

where $\boldsymbol{Y}_{\text{in},j}$ and $\boldsymbol{Y}_{\text{out},j}$ are the input and output parameter vectors (OPVs) of component j, respectively. When faults occur in a

Table 1 SNR of measured parameters of YF-20B engine test

Parameters	$\bar{X}$	ΔS	$\Delta S/\bar{X}$
Engine oxidizer mass flow rate	189.0	1.92	0.01016
Engine fuel mass flow rate	89.8	0.53	0.00590
Pressure before oxidizer injector	8.93	0.32	0.03583
Pressure at inlet of oxidizer pump	0.514	0.11	0.21401
Pressure at outlet of oxidizer pump	10.56	0.21	0.01989
Pressure at inlet of fuel pump	0.32	0.09	0.28125
Pressure at outlet of fuel pump	11.92	0.38	0.03188
Turbopump shaft speed	9840	35	0.00356
Temperature at turbine inlet	912	2	0.00219
Pressure at turbine inlet	5.69	0.08	0.01406
Pressure at turbine outlet	0.292	0.005	0.01712
Pressure before oxidizer startup valve	0.527	0.017	0.03226
Pressure before fuel startup valve	0.368	0.021	0.05707
Engine thrust	728	3	0.00412

component, the input parameter vector (IPV) and the OPV will no longer have the relationship described by Eq. (1). To describe the deviation of the OPV from the expected value computed by the component character equation, the fault factor (FF) is introduced in the component character equation, and the following formula is introduced:

$$\boldsymbol{Y}_{\text{out},j} = A_j \boldsymbol{C}_j(\boldsymbol{Y}_{\text{in},j}) \tag{2}$$

where $A_j = \text{diag}(a_1, a_2, \ldots, a_{nj})$ is the FF matrix of component j, a_i, $i = 1, 2, \ldots, nj$ is the fault factor of the ith character equation describing the deviation degree of the ith output parameter from its expected value, which is equal to 1 if the ith character equation is satisfied, and nj is the number of the output parameters of the component j.

According to Eq. (2), the OPV can be calculated from the IPV, and all output parameters can be calculated one by one in the order of component linkage. The calculation can be propagated through all components in turn. Therefore

$$\boldsymbol{Y} = \boldsymbol{H}(\boldsymbol{Y}_{itr}, A) \tag{3}$$

where $\boldsymbol{H}$ is the function formed in the parameter propagation. It is obvious that the values of a parameter obtained from different parameter propagation paths are equal, i.e.,

$$\boldsymbol{H}_1(\boldsymbol{Y}_{itr}, A) = \boldsymbol{H}_2(\boldsymbol{Y}_{itr}, A) \tag{4}$$

and the calculated value is equal to the measured value $\boldsymbol{Y}_M$ (if the measurement noise and model error are zero):

$$\boldsymbol{Y}_M = \boldsymbol{H}_3(\boldsymbol{Y}_{itr}, A) \tag{5}$$

where $\boldsymbol{H}_1$, $\boldsymbol{H}_2$, and $\boldsymbol{H}_3$ is the function formed in different parameter propagation paths, and A and $\boldsymbol{Y}_{itr}$ can be estimated using Eqs. (4), (5), and nonlinear programming, and faults can be diagnosed from the value of A.

Although there are usually few measurement parameters, resulting in difficulties of parameter estimation, experience in fault analysis indicates that the engine faults are always caused by one or two faulty components. Some fault causes can therefore initially be assumed, and then the diagnosis method based on component modules may be adopted using the inference procedure of fault hypothesis, parameter estimation, and hypothesis verification.[26]

Twenty-five categories of simulated engine faults were diagnosed using five measurement parameters for the YF-20B, and the correct diagnosis was obtained. As an example, the diagnosis results for the oxidizer pump efficiency decreasing by 30% are listed next: Hypothesis 1, the oxidizer pump (OP) being faulty: c3, 1.000 ± 5.044e-007; c4, 1.429 ± 7.720e-007; c22, 1.000 ± 5.385e-007; and optimal index, 3.4461e-007. Hypothesis 2, the fuel pump (FP) being faulty: c5, 1.000 ± 2.236e-006; c6, 1.419 ± 1.701e-006; c23, 1.000 ± 2.877e-006; and optimal index, 7.1961e-007. Hypothesis 3, the turbo (TB) being faulty: c1, 0.938 ± 7.885; c0, 0.938 ± 7.885; c25, 0.938 ± 7.885; and optimal index, 9.7306e-007. Hypothesis 4, the OP and the TB being faulty: c1, 0.9426 ± 2.203e + 228; c0, 0.9426 ± 2.203e + 228; c25, 0.942 ± 2.203e + 228; c3, 1.000 ± 4.557e + 221; c4, 1.028 ± 2.882e + 226; c22, 1.000 ± 4.342e + 221; and optimal index 4.7263e-007. (c3, FF of OP pressure equation; c4, FF of OP power equation; c22, FF of OP flow equation; c5, FF of FP pressure equation; c6, FF of FP power equation; c23, FF of FP flow equation; c0, FF of TB power equation; c1, FF of TB RT equation; and c25, FF of TB flow equation.)

In the diagnosis for oxidizer pump faults, only the fault factor of the power equation deviates from its normal value, and the efficiency deviation computed from the FF equals 30.0%, the preset value. Because oxidizer pump faults, fuel pump faults, and turbine faults in the YF-20B cannot be isolated by the five measurement parameters used here, these faults are all reasonable diagnosis results, and in the results of hypotheses 3 and 4, the confidence intervals of parameter estimation are very large. According to the value of the optimal index, the decreasing efficiency of the oxidizer pump is the most probable fault cause.

C. Engine Fault Detection and Isolation Using a Fuzzy Hypersphere Neural Network

1. *Fuzzy Hypersphere Neural Network*

The three-layer structure that implements the fuzzy hypersphere neural network is shown in Fig. 3. The input layer $\boldsymbol{A}^T = (a_1, a_2, \ldots, a_n)$ has n processing elements. There are two connections between each input node and each of the m hypersphere nodes. One connection represents the center for that dimension, and the other connection is the radius of the hypersphere. The membership function of each hypersphere node is defined as

$$b_j = 1 - \max\{0, \min[1, \gamma(\|\boldsymbol{A}_h - \boldsymbol{O}_j\| - r_j)]\} \tag{6}$$

where $\boldsymbol{O}_j^T = (o_{j1}, o_{j2}, \ldots, o_{jn})$ is the center vector of the jth hypersphere; r_j is the radius; γ is the sensitivity parameter of all hyperspheres; and $\|.\|$ denotes the module of a vector.

The connections between the hypersphere nodes and the fault class codes are binary valued. The equation for assigning the values to these connections is

$$u_{jk} = \begin{cases} 1 & \text{if } b_j \text{ is a hypersphere for class } c_k \\ 0 & \text{otherwise} \end{cases} \tag{7}$$

where b_j is the jth hypersphere node, c_k is the kth fault class node, and u_{jk} is the connect weight between b_j and c_k. Each fault class node represents the normal operating point or a fault

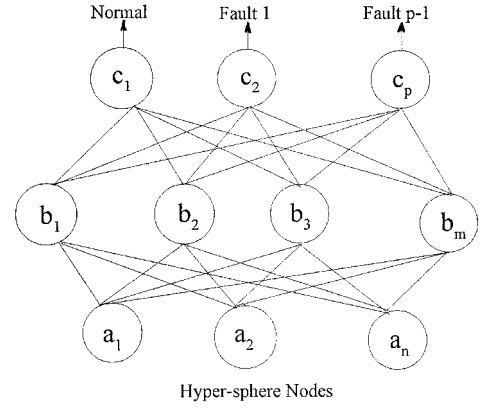

Fig. 3 Structure of fuzzy hypersphere neural network.

class. The output of the fault class node represents the degree to which the input pattern $\boldsymbol{A}$ fits within the class k. The transfer function for each of the fault class nodes joins the appropriate hyperspheres. This operation is defined by

$$c_k = \max_{j=1}^{n} b_j u_{jk} \tag{8}$$

2. Fuzzy Hypersphere Learning Algorithm

Variable hypersphere expansion: Given an ordered pair $\{\boldsymbol{A}_h, d_h\}$, where $\boldsymbol{A}_h = (a_{h1}, a_{h2}, \ldots, a_{hn}) \in I^n$ is the input pattern, and $d_h \in \{1, 2, \ldots, p\}$ is the index of one of the p classes, find the hypersphere of the same fault class, and allow expansion (if needed). The maximum size of a hypersphere is bounded by θ, a user-defined value. For the hypersphere j to expand to include $\boldsymbol{A}_h$, the following constraints must be met:

$$\|\boldsymbol{A}_h - \boldsymbol{O}_j\| < \theta \tag{9}$$

If the expansion criterion has been met for hypersphere j, then judge whether $\boldsymbol{A}_h$ is out of the hypersphere j, namely

$$\|\boldsymbol{A}_h - \boldsymbol{O}_j\| > r_j \tag{10}$$

When the two limitations have been satisfied, the hypersphere center and radius are adjusted using the following equations

$$r_j^{\text{new}} = \tfrac{1}{2}(\|\boldsymbol{A}_h - \boldsymbol{O}_j^{\text{old}}\| + r_j^{\text{old}}) \tag{11}$$

$$\boldsymbol{O}_j^{\text{new}} = \boldsymbol{O}_j^{\text{old}} + \frac{r_j^{\text{new}} - r_j^{\text{old}}}{\|\boldsymbol{A}_h - \boldsymbol{O}_j^{\text{old}}\|}(\boldsymbol{A}_h - \boldsymbol{O}_j^{\text{old}}) \tag{12}$$

Hypersphere overlap test and contraction: To determine if this expansion created any overlap, a comparison between the two hyperspheres is performed. Assume that the hypersphere j was expanded in the previous step and the hypersphere k represents another class. If there is overlap between the two hyperspheres representing different classes, it is necessary to eliminate the overlap. Three cases are examined to determine the proper adjustment.

Case 1, when

$$|r_j - r_k| < \|\boldsymbol{O}_j - \boldsymbol{O}_k\| < r_j + r_k$$

then

$$r_j^{\text{new}} = \tfrac{1}{2}(r_j^{\text{old}} - r_k^{\text{old}} + \|\boldsymbol{O}_j^{\text{old}} - \boldsymbol{O}_k^{\text{old}}\|) \tag{13}$$

$$r_k^{\text{new}} = \tfrac{1}{2}(r_k^{\text{old}} - r_j^{\text{old}} + \|\boldsymbol{O}_j^{\text{old}} - \boldsymbol{O}_k^{\text{old}}\|) \tag{14}$$

$$\boldsymbol{O}_j^{\text{new}} = \boldsymbol{O}_j^{\text{old}} + (r_j^{\text{old}} - r_j^{\text{new}})\frac{\boldsymbol{O}_j^{\text{old}} - \boldsymbol{O}_k^{\text{old}}}{\|\boldsymbol{O}_j^{\text{old}} - \boldsymbol{O}_k^{\text{old}}\|} \tag{15}$$

$$\boldsymbol{O}_k^{\text{new}} = \boldsymbol{O}_k^{\text{old}} + (r_k^{\text{old}} - r_k^{\text{new}})\frac{\boldsymbol{O}_k^{\text{old}} - \boldsymbol{O}_j^{\text{old}}}{\|\boldsymbol{O}_k^{\text{old}} - \boldsymbol{O}_j^{\text{old}}\|} \tag{16}$$

Case 2, when

$$\|\boldsymbol{O}_j - \boldsymbol{O}_k\| < r_k - r_j$$

then

$$r_j^{\text{new}} = \tfrac{1}{2}(r_j^{\text{old}} - r_k^{\text{old}} + \|\boldsymbol{O}_j^{\text{old}} - \boldsymbol{O}_k^{\text{old}}\|) \tag{17}$$

$$\boldsymbol{O}_j^{\text{new}} = \boldsymbol{O}_k^{\text{old}} + \frac{r_j^{\text{old}} + r_k^{\text{old}} + \|\boldsymbol{O}_j^{\text{old}} - \boldsymbol{O}_k^{\text{old}}\|}{2\|\boldsymbol{O}_j^{\text{old}} - \boldsymbol{O}_k^{\text{old}}\|}(\boldsymbol{O}_j^{\text{old}} - \boldsymbol{O}_k^{\text{old}}) \tag{18}$$

Case 3, when

$$\|\boldsymbol{O}_j - \boldsymbol{O}_k\| < r_k - r_j$$

then

$$r_k^{\text{new}} = \tfrac{1}{2}(r_k^{\text{old}} - r_j^{\text{old}} + \|\boldsymbol{O}_j^{\text{old}} - \boldsymbol{O}_k^{\text{old}}\|) \tag{19}$$

$$\boldsymbol{O}_k^{\text{new}} = \boldsymbol{O}_j^{\text{old}} + \frac{r_k^{\text{old}} + r_j^{\text{old}} + \|\boldsymbol{O}_j^{\text{old}} - \boldsymbol{O}_k^{\text{old}}\|}{2\|\boldsymbol{O}_j^{\text{old}} - \boldsymbol{O}_k^{\text{old}}\|}(\boldsymbol{O}_k^{\text{old}} - \boldsymbol{O}_j^{\text{old}}) \tag{20}$$

3. Engine Fault Detection Demonstration with Ground Test Data

Sensor data used for fault detection are derived with firing tests on a large liquid rocket engine, with a sampling interval time of 0.02 s.[27]

The structure parameters of the fuzzy hypersphere neural network are selected as 14 input nodes determined by the engine survey parameters, hypersphere body nodes formed to meet the demands of the real problem, and one output node representing the normal operating point. With the hypersphere expansion bias $\theta = 1$ and the sensitivity parameter $\gamma = 2.0$, the demonstration results of the engine test data are shown in Table 2.

For the normal tests, the outputs of neural network are normal. Engine test F15-1 was shut down at 275.79 s, and the neural network began to display the fault existence at 275.50 s. Therefore, the fault detection time was 0.29 s in advance of the emergency shutdown in the engine operation (Fig. 4), in which c is the membership degree and t_{hr} is the detection threshold selected by the statistical analysis of the membership degree.

4. Engine Fault Isolation

The random simulation fault classes of the rocket engine include the abnormal opening of the main oxidizer valve, the abnormal opening of the main fuel valve, and both abnormal openings at the same time. There are four classes, one for the normal operating point and the other three for the fault conditions. The number of the input nodes of the fuzzy neural network is 7, the number of the hypersphere is determined by the real problem, the number of the output nodes is 4, which

Table 2 Test data detection results

Test	Real operating condition	Detection results of the fuzzy hypersphere neural network
F15-1	Emergency after 275.80 s	Indicating fault existence in 275.50–275.80 s
N18-3	Normal	Normal
N18-4	Normal	Normal
N18-5_1	Normal	Normal
N18-5_2	Normal	Normal

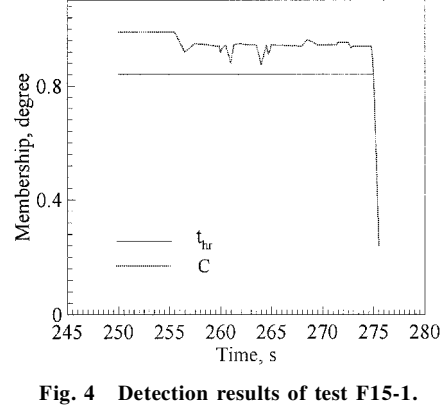

Fig. 4 Detection results of test F15-1.

Table 3 Random simulation data isolation results

Data name	Real condition	Opening degrees	Isolation results of the fuzzy hypersphere neural network	
			Class	Sensitivity
OUT	Normal		Normal	1.251
OUTDA11	Abnormal opening of main oxidizer valve	51.5	Abnormal opening of main oxidizer valve	1.168
OUTDA14	Abnormal opening of main oxidizer valve	47.0	Abnormal opening of main oxidizer valve	1.243
OUTFA7	Abnormal opening of main fuel valve	41.5	Abnormal opening of main fuel valve	1.429
OUTEA5	Both abnormal openings	53.5	Both abnormal openings	1.189
OUTEA10	Both abnormal openings	43.0	Both abnormal openings	1.187

are determined by one normal and three fault classes. With the sensitivity parameter $\gamma = 4.0$ and the expansion bias $\theta = 0.06$, there are 27 hyperspheres to be formed in the learning process. After the fuzzy neural network has been trained, random simulation data whose fault degrees are different from those of the training patterns are presented to the fuzzy neural network, and the fault isolation results are obtained as shown in Table 3, in which sensitivity is denoted as the ratio of the first output value to the second output value of the neural network. Under normal conditions the isolation result is normal. For the abnormal opening of the main oxidizer and fuel valves, simultaneously, the isolation results of the fuzzy hypersphere neural network are also correct. It is evident that the fuzzy hypersphere neural network can be successfully employed in fault and normal condition isolation for the liquid rocket engine.

D. Real-Time Verification System for Health Monitoring of LRE

A real-time verification system of FDD methods is fundamental to the development of any monitoring system's hardware and software. With such a verification system, the performance of monitoring algorithms or systems, such as reliability, real-time ability, and robustness can be evaluated in real time.

High-order dynamic nonlinear models of the engine under normal and anomalous conditions are not suitable for real-time simulation because of the very small integration steps caused by the equation stiffness.

For the YF-20B engine shown in Fig. 1, propellant inertia in the feed-system pipeline is very small and can be omitted. Hence, the stiffness of the equations is eliminated and in this way a lower-order real-time simulation model of the YF-20B engine was developed. Differential equations are still utilized to represent operational process in components such as the combustion chamber, gas generator, and turbopump, whereas static algebraic equations are used for pipe lines. The lower-order model can be described by[24]

$$\begin{aligned} \dot{\boldsymbol{z}}(t) &= \boldsymbol{f}[\boldsymbol{z}(t), \boldsymbol{y}(t), \boldsymbol{F}(t), \boldsymbol{u}(t)] \\ \boldsymbol{g}[\boldsymbol{z}(t), \boldsymbol{y}(t), \boldsymbol{F}(t), \boldsymbol{u}(t)] &= 0 \end{aligned} \tag{21}$$

where

$$\boldsymbol{z}(t) = [p_c, p_b, n]^T$$

$$\boldsymbol{y}(t) = [p_{opo}, p_{opf}, p_{oc}, p_f^l, m_o, m_{oc}, m_{ov}, m_{of}, m_f, m_{ff}, m_{fj}, m_{fg}]^T$$

$$\boldsymbol{u}(t) = [p_{ipo}, p_{ipf}]^T$$

Considering cost and performance, a Pentium-586-based real-time verification system was constructed. In the system architecture, two Pentium-586 personal computers are linked with I/O interface boards. One computer is used for running the real-time simulation models, and the other is for executing real-time monitoring algorithms.

The real-time verification system can be divided into two subsystems: A simulation system and a monitoring system. The main function of the simulation system is to simulate the transient performance of the YF-20B engine under fault conditions, redisplay the fire-test data, and display important images and/or graphics. The function of the monitoring system is to execute on-line operations of real-time fault diagnosis algorithms and output alarm signals and diagnosis results.

The real-time verification system was successfully used to demonstrate a variety of failure detection and diagnosis algorithms developed for the YF-20B engine. The running speed of the real-time simulation was well verified. The efficiency and robustness of various detection and diagnosis algorithms developed for the YF-20B engine was proved on the test system.[24]

V. Conclusions

Over the last two decades the health-monitoring techniques of LREs have progressed in system framework research, failure mode analysis, FDD algorithm development, failure control studies, and sensor technology. Important advances have been obtained in theoretical research and practical applications. However, to ensure efficient application of failure detection and diagnosis algorithms, much more research work has to be done. The research work conducted on failure detection and diagnosis for the YF-20B engine has proven to be a very helpful tool for the enhancement of the reliability of the Long March-series launch vehicles.

Acknowledgments

This work was supported by the National Natural Science Foundation, People's Republic of China, No. 59186026, and the Research Funds on Experiment Technology from Commission of Science, Technology, and Industry of National Defense, People's Republic of China, KD-96-b-011. The authors are indebted to Vigor Yang of the Pennsylvania State University for revising the manuscript.

References

[1]Nemeth, E., and Norman, A. M. , "Development of a Health Monitoring Algorithm," AIAA Paper 90-1991, July 1990.

[2]Bickmore, T. W., and Bickford, R. L., "Aerojet's Titan Health Assessment Expert System," AIAA Paper 92-3330, July 1992.

[3]Hawman, M. W., "Health Monitoring System for the SSME—Program Overview," AIAA Paper 90-1987, July 1990.

[4]Johnson, J. G., "Integrated Health Monitoring Approaches and Concepts for Expendable and Reusable Space Launch Vehicles," AIAA Paper 90-2697, July 1990.

[5]Lorenzo, C. F., and Merrill, W. C., "An Integrated Health Monitoring and Control for Rocket Engines: Need, Vision and Issues," *IEEE Control System Magazine*, Vol. 11, No. 1, 1991, pp. 42–46.

[6]Nemeth, E., Anderson, R., Maram, J., Norman, A. M., and Merrill, W. C., "An Advanced Intelligent Control System Framework," AIAA Paper 92-3162, July 1992.

[7]Song, G. Q., and Yang, R. T., "RD-170 One of Different Propulsion System of Launch Vehicles," *Journal of Rocket Propulsion of China*, No. 3, 1994, pp. 37–43.

[8]Du, T. E., and Yang, R. T., "RD-0120 Based Reusable Rocket Propulsion System," *Journal of Rocket Propulsion of China*, No. 3, 1996, pp. 6–17.

[9]Zakrajsek, J. F., "The Development of a Post-test Diagnostic System for Rocket Engines," AIAA Paper 91-2528, June 1991.

[10]Merrill, W. C., Musgrave, J. L., and Guo, T. H., "Integrated Health Monitoring and Control for Rocket Engines," NASA-TM-105763, April 1992.

[11]Tejwani, G., Dyke, D. V., and Bircher, F., "SSME Exhaust Plume Emission Spectroscopy at SSC: Recent Analytical Development and Test Results," AIAA Paper 95-2786, July 1995.

[12]Bickmore, T. W., "A Probabilistic Approach to Sensor Data Verification," AIAA Paper 92-3163, July 1992.

[13]Neppach, C. D., and Casdorph, V. A., "Sensor Failure Detection, Identification and Accommodation in A System without Sensor Redundancy," AIAA Paper 95-0011, Jan. 1995.

[14]Norman, A., Maram, J., and Coleman, P., "Development of a Real-time Model Based Safety Monitoring Algorithm for the SSME," AIAA Paper 92-3165, July 1992.

[15]Duyar, A., Eldem, V., Merrill, W. C., and Guo, T. H., "Fault Detection and Diagnosis in Propulsion Systems: A Fault Parameter Estimation Approach," *Journal of Guidance, Control, and Dynamics*, Vol. 17, No. 1, 1994, pp. 104–108.

[16]Matijevic, Z., "A Pattern-Recognition Based Expert System: A Prototype for Fault Diagnosis in a Liquid Propellant Rocket Engine," International Astronautical Federation Paper 92-0676, Aug. 1992.

[17]Whitehead, Kiech, B. E., and Ali, M., "Rocket Engine Diagnostics Using Neural Networks," AIAA Paper 90-1892, July 1990.

[18]Whitehead, B., Ferber, H., and Ali, M., "Neural Network Approach to Space Shuttle Main Engine Health Monitoring," AIAA Paper 90-2259, July 1990.

[19]Benzing, D. A., Whitaker, K. W., and Krishnakumar, K. S., "SSME Condition Monitoring Using Neural Networks and Plume Spectral Signatures," AIAA Paper 96-2824, July 1996.

[20]Bickmore, T. W., and Bickford, R. L., "Aerojet's Titan Health Assessment Expert System," AIAA Paper 92-3330, July 1992.

[21]Ali, M., and Gupta, U., "An Expert System for Fault Diagnosis in a Space Shuttle Main Engine," AIAA Paper 90-1890, July 1990.

[22]Ali, M., and Gupta, U., "Artificial Intelligence Techniques for Ground Test Monitoring of Rocket Engines," AIAA Paper 90-2384, July 1990.

[23]Chen, Q., "The Evolution of Health Monitoring Techniques of Liquid Rocket Propulsion System," *Journal of Propulsion Technology of China*, Vol. 18, No. 1, 1997, pp. 1–7.

[24]Zhang, Y., "Health Monitoring of Liquid Propellant Rocket Engines: Failure Analysis and Simulation," *Journal of Propulsion Technology of China*, Vol. 18, No. 1, 1997, pp. 8–12.

[25]Wu, J., "Fault Detection and Diagnosis for Liquid Propellant Rocket Engine," Ph.D. Dissertation, National Univ. of Defense Technology, Changsha, Hunan, PRC, Feb. 1995.

[26]Zhu, H., "Fault Detection and Diagnosis for Liquid Propellant Rocket Engine in Ground Test," Ph.D. Dissertation, National Univ. of Defense Technology, Changsha, Hunan, PRC, Dec. 1997.

[27]Huang, M., "Fault Diagnosis Study of Liquid Rocket Engine Using Neural Networks," Ph.D. Dissertation, National Univ. of Defense Technology, Changsha, Hunan, PRC, Jan. 1998.